Photochemistry and Photobiology, 2008, 84: 1244–1248

Influence of pH upon Surface-enhanced Enzyme-catalyzed Luminol Chemiluminescence at Vicinity of Nanoscale-corrugated Gold and Silver Films

Meigui Ou[1], Guowei Lu[1], Hong Shen[2], Armel Descamps[1], Christophe André Marquette[3], Loïc Jacques Blum[3], Stéphane Roux[4], Olivier Tillement[4], Bolin Cheng[2] and Pascal Perriat*[1]

[1]MATEIS, INSA-Lyon, Université de Lyon, Villeurbanne, France
[2]Beijing National Laboratory for Condensed Matter Physics, Institute of Physics, Chinese Academy of Sciences, Beijing, China
[3]Laboratoire de Génie Enzymatique et Biomoléculaire, Université Claude Bernard Lyon 1, Villeurbanne, France
[4]Laboratoire de Physico-Chimie des Matériaux Luminescents, Université Claude Bernard Lyon 1, Villeurbanne, France

Received 16 October 2007, accepted 5 February 2008, DOI: 10.1111/j.1751-1097.2008.00350.x

ABSTRACT

Au and Ag biochips were fabricated to investigate the influence of pH upon the chemiluminescence (CL) of luminol at vicinity of surface-adsorbed peroxidase. A nanoscaled-corrugation of the metal induces an enhancement of the luminol CL which is maximal in the pH range favoring peroxidase catalysis and greater for gold than for silver. This is the proof that, in the CL process, the reactions involving peroxidase are surface-enhanced near corrugated surfaces.

INTRODUCTION

Chemiluminescence (CL) is extensively studied as an important analytic technique in biotechnology and medical diagnostics due to its simplicity, rapidity and high sensitivity (1). Among the reactions producing CL, these luminol-involved CL reactions have attracted some considerable attention and much effort was made to increase the efficiency of the reaction. On one hand, the investigation of efficient catalysts for CL reactions was carried out, including metal ions, metal complexes and enzymes (2). On the other hand, gold particles (3) and silver films (4) were recently observed to strongly enhance CL either by an increase of the local electromagnetic field (5) or by an electronic interaction between metal and adsorbate (*i.e.* a chemical effect) (6). We recently showed that, in fact, CL was more greatly enhanced when the two kinds of catalysts were applied together, *i.e.* when the CL of the luminol/hydrogen peroxide (H_2O_2) system was catalyzed by an enzyme (the peroxidase) in the simultaneous presence of a metal-corrugated film (7). We also proved that the enhancing mechanism of luminol CL is not related to plasmon-assisted processes but originates from catalytic properties of the metal induced by corrugation (8,9). This paper aims to determine which steps among the numerous reactions involved in luminol CL are concerned by metal catalysis. A lot of parameters were already studied to optimize the reactive conditions between luminol and hydrogen peroxide: the activity of peroxidase, the pH, the luminol concentration and the presence of O_2 and N_2 (2,10). Among these factors, pH which is involved in the light emitting steps of luminol oxidation was found to be one of the more important (10). It was reported that light emission is not detected below pH 5.6 and that CL intensity reaches a maximum in neutral and alkaline solution (11–14).This is the reason why the paper focuses more precisely on the influence of pH upon the catalytic enhancement of luminol CL obtained at vicinity of metal films. In the experiments presented, horseradish peroxidase has been fixed on the films *via* a biotinylated peptide with a length sufficiently small (3.5 nm) to ensure a significant catalytic effect without correlative light emission quenching by metal (15). Also the chemical nature of the metal (Au, Ag) was varied for a better understanding of the mechanisms involved.

MATERIALS AND METHODS

Fabrication of metal films. The noble metal films used in this paper were all prepared on quartz substrate using a pulsed laser deposition (PLD) technique in vacuum (~10 Pa). In the homemade apparatus, a foil of the compound to deposit (used as a target) is placed at a distance of a quartz substrate of about 40 mm. A XeCl excimer laser (308 nm, 17 ns full width at half maximum) operating at 1 Hz repetition rate is then focused onto the target. Two main factors permit to easily control the properties of metal films: the film thickness and the substrate temperature during deposition. Commonly, noble metal films can change from a cluster-like material to a bulk-like one when increasing thickness, the surface plasmon resonance band redshifting accordingly before finally disappearing. Also, the metal film can change from a bulk-like material to a cluster-like one when increasing the deposition substrate temperature: this is correlated to the appearance of a surface plasmon resonance (SPR) band followed by further blueshift as shown in previous work (13). So, Au and Ag thin films with various properties can be easily prepared using PLD technique by controlling either the deposition thickness or the temperature. In our experimental conditions, the thickness is kept constant (25 nm) and the temperature is the tunable parameter. Additionally, before Ag deposition, a 1 nm thick $BaTiO_3$ layer was

*Corresponding author email: Pascal.perriat@insa-lyon.fr (Pascal Perriat)

deposited onto quartz substrate to enhance the adhesion between Ag and substrate. Furthermore, AuAg alloy metal films were prepared using the target technique. This technique uses a rotating disk made of Au and Ag fan-shaped foils, the Au/Ag ratio of alloy films being controlled by adjustment of fan-shaped areas ratio.

Atomic force microscopy. Atomic force microscopy (AFM) images of films were collected using Digital Instruments Nanoscope Di3100 and operating in tapping mode. Roughness of samples was defined as the standard deviation of the height value within a box cursor with a size of 250×250 nm^2 and a resolution of 256×256. AFM images of Au films prepared at 30°C and 600°C are shown in Fig. 1a and c. They present smooth (bulk-like) and corrugated (cluster-like) surfaces, respectively. Figure 1b and d give similar images of flat and corrugated Ag films prepared, respectively, at 30°C and 600°C. All the characteristics of the films are given in Table 1.

Chemiluminescence measurement. As displayed in Fig. 2, first, the films were immersed during 2 h in a solution (1 mg mL^{-1}) of tri-thiolated polypeptides modified with a biotin molecule at their N-terminal end. The films were then washed to remove all unbound molecules. In a second step, the treated films were immersed for 20 min in Veronal Buffer Saline (VBS) containing additional 1% bovine serum albumin and 0.1% polyoxyethylenesorbitan monolaurate (Tween 20) and finally incubated with peroxidase labeled streptavidin (1 μg mL^{-1}) for 30 min. The peroxidase labeled streptavidin has a globular size of 6–10 nm and the distance between peroxidase and metal is adjusted by the peptide chain length. Here, a peptide containing 11 amino acids was used to get a separation distance of about 3.5 nm between metal and peroxidase. The films were then divided in eight compartments separated by a hydrophobic layer. Each of the eight compartments was then filled with a VBS solution containing 220 μM luminol and additives agents favoring its CL (500 μM H_2O_2 and 200 μM *p*-iodophenol). The pH of each compartment was then adjusted to values varying from 7 to 12 (7, 8, 8.5, 9, 10, 11, 11.5 and 12) by addition of suitable quantities of NaOH (5 *N*) or HCl (6 *N*). CL measurements were then taken with a −30°C cooled CCD camera (Intelligent Dark Box II; Fuji Film). The light emitted by the luminol brought at peroxidase vicinity was integrated for 10 s. The images obtained were quantified and the results were given in arbitrary units (a.u.).

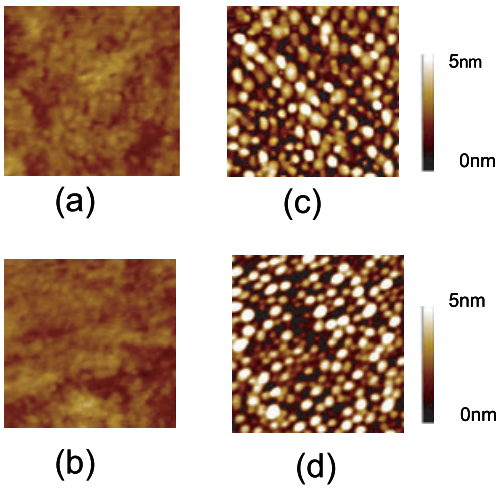

Figure 1. AFM images (area of 500×500 nm^2) of "bulk-like" Au (a) and Ag (b) films prepared at room temperature and "cluster-like" Au (c) and Ag (d) films prepared at high temperature.

X-ray photoelectron spectroscopy. X-ray photoelectron spectroscopy analysis was carried out at the "Institut de Recherche sur la Catalyse" with a VG Scientific ESCA LAB 200 R using a 220 W Al Kα radiation (1486.6 eV). Spectra relative to C1s, O1s, N1s, S2p, Si2s, Au4f7/2 and Ag3d photoelectron peaks were measured at binding energies around, respectively, 284.6, 531.0, 399.4, 162.8, 153.3, 83.7 and 367.9 eV. The spot size on sample is of 400×1000 μm^2. From the areas of the different elements' peaks, the peptide density was determined according to a method previously explained (8). This density is given in Table 1. For all the composition (Au, Ag and AuAg), the peptide density is comprised between ~1 and 4 peptide nm^{-2}. For a given composition the grafting density is slightly greater for cluster-like films than for bulk-like ones. Also the peptide density is higher for samples containing silver than for those made in pure gold. Whereas thiols have similar affinity for gold and silver (16), weaker interactions occur between nitrogen and silver than between nitrogen and gold (17). Then peptides which contain a large amount of N tend more to lie down along gold surfaces than silver ones explaining why a greater peptide density can be grafted in the case of silver. A similar result was already obtained for adsorption of disulfide-modified polyacrylamides to gold or silver surfaces (18). After peroxidase labeled streptavidin coating, the metal content measured by XPS is strongly decreased due to the size of the protein (6–10 nm). The mean free path of electrons in organic compounds is of a few nanometers (≈5 nm). Assuming that when the surface is coated by both peptide and peroxidase labeled streptavidin (with a total length of ≈11.5 nm) the metal is no more visible, the proportion of the surface coated by streptavidin can be evaluated from the metal content decrease observed upon streptavidin coating. Whatever the sample analyzed (Au or Ag) and the morphology of the metal substrate (flat or rough), the proportion of the surface coated by peroxidase labeled streptavidin is of around 0.55 (Table 1). Compared with the maximal density obtained in the case of a hexagonal paving (0.90), the paving density of peroxidase labeled streptavidin is then of 60% of the maximal one. That means that all the peptide densities are sufficient to ensure a homogeneous peroxidase coating. It is certainly due to the fact that a biotinylated site is available at positions every nanometer apart or less whereas strepatvidin labeled peroxidase has a size of 6–10 nm.

RESULTS AND DISCUSSION

The reaction of luminol/H_2O_2 catalyzed by peroxidase involves two principal stages: (1) the first one is the enzymatic stage appearing as the sequence of the following reactions (R) (19):

$$P + H_2O_2 \rightarrow PI + H_2O$$

$$PI + L \rightarrow PII + L^{\bullet -}$$

$$PII + L \rightarrow P + L^{\bullet -} + H_2O$$

where P, PI and PII are peroxidase and two intermediate complexes, respectively; L and $L^{\bullet -}$ are luminol and the product of free-radical single-electron oxidation, respectively. (2) The

Table 1. Characteristics of the samples studied.

	Temperature of elaboration (°C)	Roughness (nm)	Particle size (nm)	Peptide density (peptide/nm^2)	Average distance between two peptides (nm)	Surface density of peroxidase labeled streptavidin
Au film	30	0.3	–	1.3 ± 0.4	0.9 ± 0.3	0.50 ± 0.15
	600	1.9	35	1.6 ± 0.5	0.8 ± 0.2	0.55 ± 0.15
Ag film	30	0.3	–	2.5 ± 0.3	0.6 ± 0.2	0.55 ± 0.15
	600	3.6	37	3.2 ± 0.6	0.6 ± 0.3	0.55 ± 0.15
AuAg film	500	4.4	32	2.5 ± 0.5	0.6 ± 0.2	–

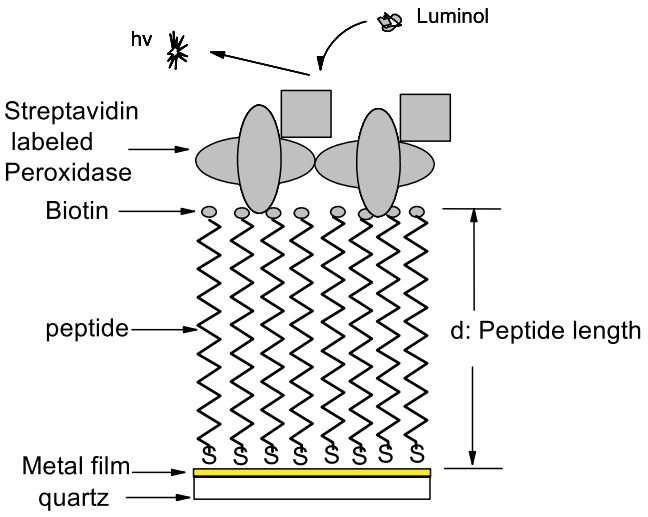

Figure 2. Schematic representation of the process involved in the luminol chemiluminescence catalyzed by peroxidase near metal surface (Au, Ag or AuAg).

second stage involves the transformation from $L^{\bullet -}$ to 3-aminophthalate in an excited state which results in light emission (20). In presence of peroxidase (2), luminol CL is maximal for pH ranging between 8 and 9 whereas in absence of this catalyst (21,22), the maximum of CL locates at 10–11 pH value.

In this study, the influence of pH upon luminol/hydrogen peroxide CL was first investigated for reactions occurring near flat surfaces. Figure 3 which displays the CL intensity as a function of pH on flat glass, Au and Ag films clearly shows two different types of behavior for, on one hand, the glass support and, on the other hand, the metal films. For glass, CL is maximal for pH comprised between 8.5 and 9 and is almost equal to zero for pH superior to 10. This indicates that at vicinity of glass, peroxidase acts effectively as a catalyst for the reactions responsible for luminol CL. This result is in agreement with the fact that peroxidase was already found to catalyze CL at vicinity of glassy carbon electrodes (2). On the contrary, in the case of Ag, CL is low at pH 8.5 and is maximal in the pH range comprised between 9 and 11. This indicates that the catalytical activity of peroxidase is strongly decreased when the enzyme is fixed on flat silver film which is probably due to a light emission quenching not yet completely negligible at a distance of around 10 nm from the metal. Similarly, a CL maximum is observed at pH 10 at vicinity of flat gold. However, a second maximum is also present in the pH range 8–8.5 and it appears that luminol CL is greater than near silver. All these observations are consistent with the fact that gold was already pointed out as a better catalyst than silver for surface-enhanced CL (8). Indeed, the films studied here are not completely flat but characterized by a small corrugation of the order of 0.3 nm, sufficient to induce a small but measurable CL enhancement. The present result could then be a confirmation of the difference in catalytic properties of the metals and a first indication that the reactions catalyzed by nano-corrugated gold are the ones which are preferably enhanced for pH around 8.5. In absence of any corrugation, one could reasonably think that, as in the case of Ag, CL should be negligible in this pH range near Au. This assumption schematized in Fig. 3a by the dotted line is justified by the fact

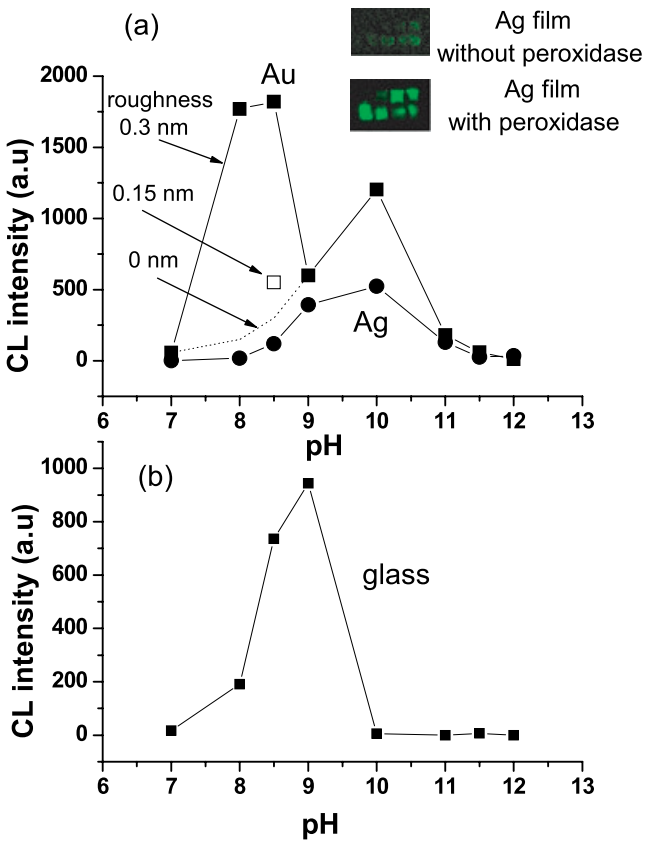

Figure 3. Effect of pH upon the chemiluminescence of the luminol–H_2O_2 system catalyzed by peroxidase at vicinity of flat Au and Ag films (a) and glass (b) for different roughness. Inset: CL at different pH on flat Ag films in presence or in absence of peroxidase; from left to right, pH in first row corresponds to 7, 8, 8.5 and 9 and in second row to 10, 11, 11.5 and 12.

that for a flat gold film with a smaller roughness (0.15 instead of 0.3 nm), the CL measured at pH 8.5 is strongly decreased: from 1800 in arbitrary units for a roughness of 0.3 nm to 600 for a roughness of 0.15 nm.

Figure 4 gives the CL intensity as a function of pH on cluster-like Au and Ag films. The first observation is that, for

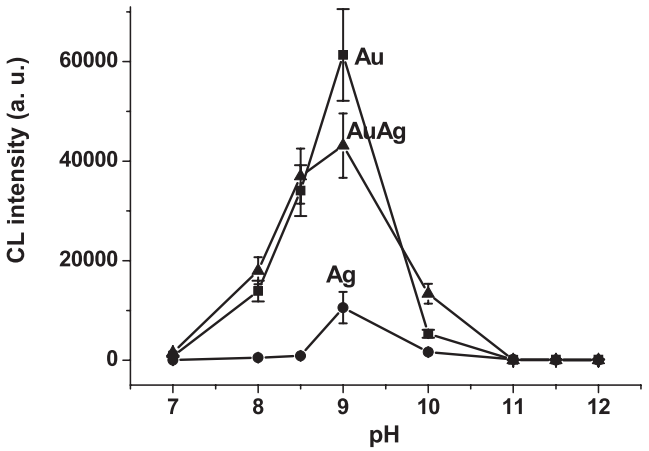

Figure 4. Effect of pH upon the chemiluminescence of the luminol–H_2O_2 system catalyzed by peroxidase at vicinity of corrugated (cluster-like) Au, Ag and AuAg films. Corrugation induces an enhancement of the chemiluminescence at pH 9.

both metals, CL is systematically greater than in the case of flat films: for gold for instance CL increases from 60 to 800 (in a.u.) at pH 7 and from 20 to 130 at pH 11.5. This shows that some nano-corrugation in metal induces a significant CL enhancement at all the pH values studied and not only at pH 8.5 (the pH fixed in our previous works) (7,9,15). Moreover whereas CL presents a maximum at pH 9 for both metals, the signal is much more important for nano-corrugated gold which confirms clearly that it is a better catalyst than corrugated silver. Concerning silver, very striking is that the position of the CL maximum between the two morphologies of the films is pH-dependent: whereas in absence of corrugation, CL is maximal at around pH 10 (a range favoring the reactions taking place without help of peroxidase), it is maximal at pH 9 in presence of corrugation. As pH 9 increases peroxidase activity, this could prove that corrugation enhances preferentially the reactions involving the enzyme. This conclusion is reinforced by the case of gold for which the maximal CL observed is also shifted in the exact range of pH (8.5–9) favoring peroxidase-related reactions. In absence of peroxidase, Zhang *et al.* (3) found that gold particles significantly enhance CL of the luminol–H_2O_2 system at pH 12. They suggest that the O–O bond of H_2O_2 is broken up into double $OH^{\bullet}$ radicals by virtue of gold catalysis facilitating then the formation of luminol radical $L^{\bullet -}$. Our present experiments confirm this result since at pH 12 (a pH at which peroxidase does not act as a catalyst) they also evidence a CL enhancement induced by corrugation. Indeed, luminol CL increases of around one order of magnitude from 10 ± 3 in arbitrary units at vicinity of flat gold (Fig. 3) up to 130 ± 40 near corrugated gold (Fig. 4). However, when peroxidase is grafted on corrugated gold, luminol CL is maximal at pH 9 (the pH enhancing catalysis by peroxidase) and strongly greater than at pH 12: 61 300 instead of 130 in the same arbitrary units. The reactions involving peroxidase are then also surface-enhanced with an enhancement factor of two orders of magnitude (at pH 9, CL increases from 600 at vicinity of flat gold up to 61 300 near corrugated gold). According to the reactions (R), the catalytic mechanisms involving peroxidase require the presence of hydrogen peroxide. It is then possible that metal catalysis could again arise from an enhanced electron transfer from metal clusters to adsorbed H_2O_2 (3). This process, known as particle-mediated transfer (23), produces some key intermediate hydroxyl and hydroperoxide radicals favoring the formation of complexes containing peroxidase and/or that of luminol radical in presence of these complexes. This interpretation is based on several reports evidencing the formation of active oxygen-containing reactant intermediates such as $OH^{\bullet}$ or $O_2^{\bullet}$ when gold particles are used as catalysts (24,25). A second mechanism acting in conjunction with peroxidase catalysis could be caused by the decrease of the redox potential of luminol at vicinity of corrugated gold. Such a shift which facilitates luminol oxidation in presence of catalyzing peroxidase was already evidenced by our team when luminol is directly fixed on a gold cluster (26).

An AuAg-corrugated film was finally compared with the corrugated Au and Ag films studied in the paper. Despite the large silver content of this film (50%), the catalytic efficiency of the AuAg film more closely resembles that of the Au one and induces even greater CL for all pH except 9. We suggest that this result could be explained by the difference in roughness between the two samples, Au films having a roughness of 1.9 nm and AuAg ones a larger one of 4.4 nm. Indeed, the catalytic enhancement which arises from the modification of thermodynamic properties at vicinity of highly curved surfaces (27) is expected to increase with roughness and should then be more pronounced for the film with the highest roughness (8). The present results show then that the catalytic process is a complex mechanism with an efficiency depending mainly on two parameters: the nature of the metal and the roughness.

For all the corrugated metals and alloy studied here (Au, Ag and AuAg), the pH inducing the greatest CL is always 9. This last value slightly differs from the optimal pH 8.5 usually found in absence of metal-induced catalysis (2) as in assays where peroxidase is directly deposited on a glass substrate (Fig. 3b). For the luminol/hydrogen peroxide system catalyzed by peroxidase, the optimal pH leading to greatest CL depends then on the nature and the morphology of the substrate.

In summary, different metal and alloy corrugated films (Au, Ag and AuAg) were fabricated to study the pH conditions leading to the maximal surface-enhancement of the peroxidase-catalyzed CL of the luminol–H_2O_2 system. For all metals, an optimal pH of 9 is found, a value which belongs to the range which favors the reactions catalyzed by peroxidase. This is the proof that, in the CL process, the reactions involving peroxidase are surface-enhanced by the presence of metal corrugation. This also indicates that the catalytic mechanisms could consist of an enhanced electron transfer from metal clusters to adsorbed H_2O_2. In this context, nanoscale-corrugated gold appears as a better catalyst than silver for surface-enhanced CL and the paper finally gives some keys for practical improvement of CL assays.

Acknowledgements—We are grateful for the financial support from the National Natural Science Foundation of China (Grant 10574157), the National Basic Research Program of China (Grant 2006cb302900) and the AFCRST of France.

REFERENCES

1. Niazov, T., V. Pavlov, Y. Xiao, R. Gill and I. Willner (2004) DNAzyme-functionalized Au nanoparticles for the amplified detection of DNA or telomerase activity. *Nano Lett.* **4**, 1683–1687.
2. Marquette, C. A. and L. J. Blum (2002) Recent developments in luminol–H_2O_2 chemiluminescence based flow injection assays. *Recent Res. Devel. Pure Applied Anal. Chem.* **4**, 9–20.
3. Zhang, Z. F., H. Cui, C. Z. Lai and L. J. Liu (2005) Gold nanoparticle-catalyzed luminol chemiluminescence and its analytical applications. *Anal. Chem.* **77**, 3324–3329.
4. Aslan, K., S. N. Malyn and C. D. Geddes (2006) Multicolor microwave-triggered metal-enhanced chemiluminescence. *J. Am. Chem. Soc.* **128**, 13372–13373.
5. Moskovits, M. (1985) Surface-enhanced spectroscopy. *Rev. Mod. Phys.* **57**, 783–826.
6. Otto, A. (2005) The "chemical" (electronic) contribution to surface-enhanced Raman scattering. *J. Raman Spectrosc.* **36**, 497–509.
7. Lu, G. W., B. L. Cheng, H. Shen, Z. H. Chen, G. Z. Yang, C. A. Marquette, L. J. Blum, O. Tillement, S. Roux, G. Ledoux, A. Descamps and P. Perriat (2006) Influence of the nanoscale structure of gold thin films upon peroxidase-induced chemiluminescence. *Appl. Phys. Lett.* **88**, 023903.
8. Ou, M. G., G. W. Lu, H. Shen, A. Descamps, C. A. Marquette, L. J. Blum, G. Ledoux, S. Roux, O. Tillement, B. Cheng and P. Perriat (2007) Catalytic performance of nanoscale-corrugated gold and silver films for surface-enhanced chemiluminescence. *Adv. Funct. Mater.* **17**, 1903–1909.

9. Shen, H., G. Lu, M. Ou, C. A. Marquette, G. Ledoux, S. Roux, O. Tillement, P. Perriat, B. Cheng and Z. Chen (2007) How the morphology of biochips roughness increases surface-enhanced chemiluminescence. *Chem. Phys. Lett.* **439**, 105–109.
10. Cui, H., Y. Xu and Z. F. Zhang (2004) Multichannel electrochemiluminescence of luminol in neutral and alkaline aqueous solutions on a gold nanoparticle self-assembled electrode. *Anal. Chem.* **76**, 4002–4010.
11. Osman, A. M., G. Zomer, C. Laane and R. Hilhorst (2000) Comparative studies of the chemiluminescent horseradish peroxidase-catalysed peroxidation of acridan (GZ-11) and luminol reactions: Effect of PH and scavengers of reactive oxygen species on the light intensity of these systems. *Luminescence* **15**, 189–197.
12. Badocco, D., P. Pastore, G. Favaro and C. Maccà (2007) Effect of eluent composition and pH and chemiluminescent reagent pH on ion chromatographic selectivity and luminol-based chemiluminescence detection of CO_2^+, Mn^{2+} and Fe^{2+} at trace levels. *Talanta* **72**, 249–255.
13. Wang, C. M. and H. Cui (2007) Electrogenerated chemiluminescence of luminol in neutral and alkaline aqueous solutions on a silver nanoparticle self-assembled gold electrode. *Luminescence* **22**, 35–45.
14. Oosthuizen, M. M. J., M. E. Engelbrecht and H. Lambrechts (1997) The effect of pH on chemiluminescence of different probes exposed to superoxide and singlet oxygen generators. *J. Biolumin. Chemilumin.* **12**, 277–284.
15. Lu, G. W., H. Shen, B. Cheng, Z. Chen, C. A. Marquette, L. J. Blum, O. Tillement, S. Roux, G. Ledoux, M. G. Ou and P. Perriat (2006) How surface-enhanced chemiluminescence depends on the distance from a corrugated metal film. *Appl. Phys. Lett.* **89**, 223128.
16. Buttry, D. A. and M. D. Ward (1992) Measurement of interfacial processes at electrode surfaces with the electrochemical quartz crystal microbalance. *Chem. Rev.* **92**, 1355–1379.
17. Michota, A., A. Kudelski and J. Bulowska (2002) Molecular structure of cysteamine monolayers on silver and gold substrates comparative studies by surface-enhanced Raman scattering. *Surf. Sci.* **502–503**, 214–218.
18. Munro, J. C. and C. W. Frank (2003) Adsorption of disulfide-modified polyacrylamides to gold and silver surfaces as cushions for polymer-supported lipid bilayers. *Polymer* **44**, 6335–6344.
19. Alpeeva, I. S. and I. Y. Sakharov (2007) Luminol oxidation catalyzed by Royal Palm leaf peroxidase. *Appl. Biochem. Microbiol.* **43**, 25–28.
20. Thorpe, G. H. G., L. J. Kricka, S. R. Moseley and T. P. Whitehead (1985) Phenolsas enhancers of the chemiluminescent horseradish peroxidase-luminol–hydrogen peroxide reaction: Application in luminescence-monitored enzyme immunoassays. *Clin. Chem.* **31**, 1335–1341.
21. Zhang, H. L. and H. A. Mottola (1996) Carbon dioxide-enhanced luminol chemiluminescence in the absence of added oxidant. *Analyst* **121**, 211–218.
22. Krasowska, A., D. Rosiak and K. Szkapiak (2000) Chemiluminescence detection of peroxyl and comparison of antioxidant activity of phenolic compounds. *Curr. Top. Biol.* **24920**, 89–95.
23. Henglein, A. (1993) Physicochemical properties of small metal particles in solution: "Microelectrode" reactions, chemisorption, composite metal particles, and the atom-to-metal transition. *J. Phys. Chem.* **97**, 5457–5471.
24. Grisel, R., K. J. Weststrate, A. Gluhoi and B. E. Nieuwenhuys (2002) Catalysis by gold nanoparticles. *Gold Bull.* **35**, 39–45.
25. Overbury, S. H., L. Ortiz-Soto, H. G. Zhu, B. Lee, M. D. Amiridis and S. Dai (2004) Comparison of Au catalysts supported on mesoporous titania and silica: Investigation of Au particle size effects and metal-support interactions. *Catal. Lett.* **95**, 99–106.
26. Roux, S., B. Garcia, J. L. Bridot, M. Salomé, C. Marquette, L. Lemelle, P. Gillet, L. Blum, P. Perriat and O. Tillement (2005) Synthesis, characterization of dihydrolipoic acid capped gold nanoparticles, and functionalization by the electroluminescent luminol. *Langmuir* **21**, 2526–2536.
27. Gibbs, J. (1928) *Collected Works*. Yale University Press, New Haven, CT.